

DETERMINING THE STRENGTH OF REFRACTORIES
 WITH ACCOUNT TAKEN OF THE TRUE RELATION
 BETWEEN THE STRESS AND DEFORMATION

G. A. Gogotsi, Ya. L. Grushevskii,
 and A. A. Kurashvskii

UDC 666.76.017:620.174

The data about the behavior of a material under a load required [1] for assessing its thermal strength were obtained in flexural tests on a modified RM-101 tensile testing machine which was equipped with a reverser 1 (Fig. 1) with load-forming supports (Fig. 2; $a = 22 \text{ mm}$, $L = 89.2 \text{ mm}$). The force applied to the specimen was measured with a ring dynamometer 2 provided with a 1-IGM-type indicator 3 giving readings in microns (see Fig. 1). The readings were recorded by means of a tensoresistor 4 bonded to an elastic element and connected over a strain-gage amplifier 5 with two-coordinate PDS-012M-type potentiometers 6 which were used for recording the deformation diagram.

The deflection of the specimen was measured with an extensometer 7 the response element of which is a 6MKh1S mechanotron with a maximum rod travel of 200μ [2].

The deformation was recorded with a 2PKP-10-100GB-type tensoresistor 8 bonded to the surface of the specimen. The measurements were repeated in order to render them more reliable.

The investigation was carried out with several refractories of substantially dissimilar compositions (Table 1).

The tests yielded the deformation diagrams of all materials concerned in the coordinates $F = f(\epsilon)$. Typical diagrams of the materials are shown in Fig. 3 and the limiting deformations are given in Table 2. The diagrams in Fig. 3 are characterized by differences in the relation between the force and the deforma-

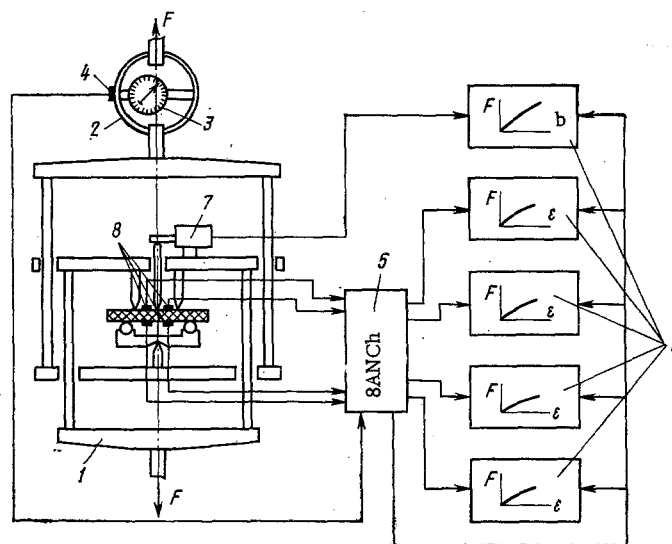


Fig. 1. Apparatus for strength measurements.

Institute of Problems of Strength of the Academy of Sciences of the Ukrainian SSR. Translated from *Ogneupory*, No. 1, pp. 45-50, January, 1976.

©1976 Plenum Publishing Corporation, 227 West 17th Street, New York, N.Y. 10011. No part of this publication may be reproduced, stored in a retrieval system, or transmitted, in any form or by any means, electronic, mechanical, photocopying, microfilming, recording or otherwise, without written permission of the publisher. A copy of this article is available from the publisher for \$15.00.

TABLE 1. The Characteristics of the Specimens

Specimen No.	Material	Composition	Porosity, %	Density, g/cm ³	Specimens produced by	Heat treatment temperature, °C	Average cross section of the specimens, mm
1	Translucent alumina	Al ₂ O ₃ + 0,1% MgO	0	3,97	Slip casting	1950	11,5 × 5,5
2	Composite alumina	Al ₂ O ₃ + 1% TiO ₂ + 7% Al ₂ O ₃	7	3,45	Semidry molding	1650	12 × 8,2
3	Alumina with zircon	Al ₂ O ₃ + 15% ZrSiO ₄	23	3,45	Slip casting	1750	12,5 × 7,9
4	Unfired zirconia	ZrO ₂ + 4% CaO + 4% H ₃ PO ₄	17	4,40	Semidry molding	300	16,2 × 10,0

TABLE 2. The Mechanical Characteristics of the Materials

Specimen No.	Limiting deformation, rel. units		Ultimate tensile strength $\sigma_{u,b}$, kg/cm ²	Elastic modulus, kg/cm ²		Measure of brittleness χ
	in tension $\epsilon_t \cdot 10^4$	in compression $\epsilon_c \cdot 10^4$		in tension $\epsilon_t \cdot 10^{-6}$	in compression $\epsilon_c \cdot 10^{-6}$	
1	4,75	4,75	1916	4,05	4,05	1,0
2	2,65	2,60	615	2,64	2,64	0,85
3	9,58	7,35	470	0,94*	1,21*	0,40
4	3,20	2,49	31,5	0,19*	0,24*	0,38

*In Fig. 4 the difference in the moduli is not discernible.

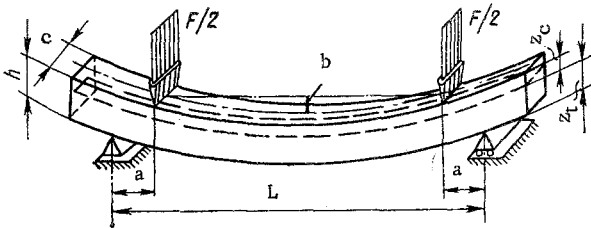


Fig. 2. Schematic presentation of the load application on the specimen. The neutral plane of the beam is shown by the broken line.

tion of the material in the extension and compression zones of the specimen. In the case of materials showing nonlinearity in the deformation diagrams residual deformation develops even at loads below the limiting ones.

Some workers [3-5, etc.] have already drawn attention to the stiffness of brittle materials at normal and notably at high temperatures. According to some published results [4, 5], the disregard of nonlinearity when interpreting the diagrams results in significant errors in the calculation of the strength. In some cases [4, 5, etc.] the workers concerned studied materials which deform nonlinearly but failed to take

account of the fact that for a brittle material the resistance to extension may differ from the resistance to compression.

For the evaluation of the results obtained in the present investigation the writers developed a procedure in which account is taken of both, the nonlinearity of the deformation diagrams and the difference in the resistance to extension and compression. The procedure is based on the principle [6, p. 402] of plotting the stress-strain curve on the basis of the experimentally determined relation between the bending moment and the deformation of the outer fibres of the specimen.

Consider the equations of equilibrium of a beam:

$$\int_{z_t}^{z_c} \sigma(z) b dz = 0, \quad (1)$$

$$\int_{z_t}^{z_c} \sigma(z) z b dz = M, \quad (2)$$

where $M = Fa$ is the bending moment, kg · cm; z is a coordinate which is measured from the neutral plane of the specimen, cm.

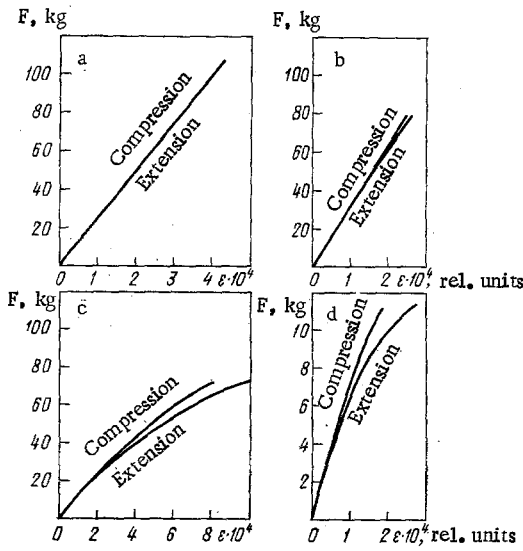


Fig. 3

Fig. 3. Original diagrams of the deformation of the specimens in the coordinates force F - deformation ε : a-d) for specimens Nos. 1-4 respectively.

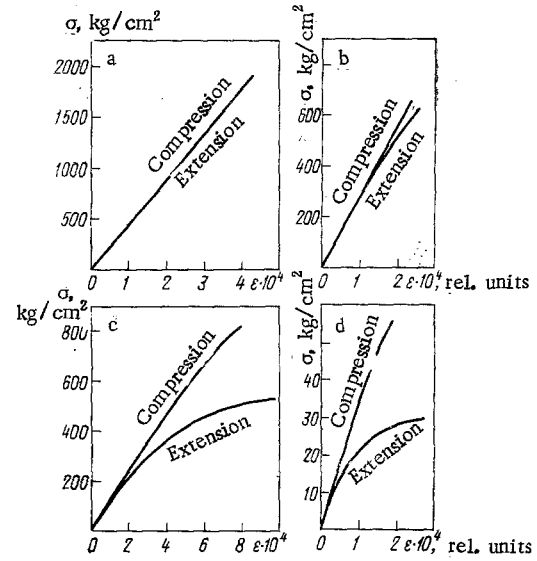


Fig. 4

Fig. 4. Deformation diagrams of the refractories in the coordinates ultimate strength σ - deformation ε : a-d) for specimens Nos. 1-4 respectively.

Here and elsewhere the subscripts t and c denote quantities which relate to the extended and compressed fibres of the specimen respectively. The remaining notation is given in Fig. 2. Assuming that the hypothesis of plane sections is valid in the deformation of the specimen it follows that

$$\varepsilon = z/\rho, \quad (3)$$

where ρ is the radius of the curvature of the neutral plane of the beam, cm.

Let the variable z in Eq. (1) and (2) be substituted by ε in accordance with Nadai's method [6] followed by the differentiation of both equations in terms of $\varepsilon_t + \varepsilon_c$. Subsequent manipulations will give the equations which define the stress in the outer fibres:

$$\sigma_p = \frac{a}{bh^2} \left(F + \frac{1}{2} \cdot \frac{\varepsilon_m}{\varepsilon_m'} \right) \left(1 + \frac{\varepsilon_c'}{\varepsilon_t'} \right), \quad (4)$$

$$\sigma_c = \frac{a}{bh^2} \left(F + \frac{1}{2} \cdot \frac{\varepsilon_m}{\varepsilon_m'} \right) \left(1 + \frac{\varepsilon_t'}{\varepsilon_c'} \right), \quad (5)$$

where $\varepsilon_m = (\varepsilon_t + \varepsilon_c)/2$ is the mean deformation of the specimen, and the prime denotes the derivative in terms of the force (e.g., $\varepsilon_t' = d\varepsilon_t/dF$).

Using Eq. (4), the tensile deformation diagram of the specimen can be plotted from the experimental curves of $F = F(\varepsilon_t)$ and $F(\varepsilon_c)$ for an arbitrary relation between the stress and deformation. The peak stress in the curve of the tensile deformation will represent the bending strength $\sigma_{u,b}$ of the material.

The results of the calculation of the ultimate bending strength $\sigma_{u,b}$ of the materials concerned here are given in Table 2. The calculations from Eq. (5) only give part of the diagram of the deformation by compression since in the zone of extension the destruction of the specimen sets in long before the deformation of the compressed fibres reaches limiting values so that the quantity $\sigma_{u,c}$ is not of interest.

The deformation diagrams plotted as $\sigma = f(\varepsilon)$ from the function $F = F(\varepsilon)$ in Fig. 3 is shown in Fig. 4. Note that the diagrams in Fig. 4 represent four types of deformation diagrams characteristic for brittle materials [7]. The diagram in Fig. 4a, for example, is of type I because the stress-deformation function

TABLE 3. Results of the Bending Strength Calculations

Specimen No.	$\sigma_{u,r}$, kg/cm ²	σ_N , kg/cm ²	σ_D , kg/cm ²	σ_{lim} , kg/cm ²	Relative error, %		
					$\frac{\sigma_N - \sigma_{u,t}}{\sigma_{u,t}} \times 100$	$\frac{\sigma_D - \sigma_{u,t}}{\sigma_{u,t}} \times 100$	$\frac{\sigma_{lim} - \sigma_{u,t}}{\sigma_{u,t}} \times 100$
1	1916	1916	1916	1916	0	0	0
2	615	631	646	649	2,6	5,0	5,5
3	470	576	595	671	21,2	26,1	42,7
4	31	40	41	46	27	31	47

TABLE 4. Results of the Calculations of the Elastic Modulus, kg/cm²

Specimen No.	$E_t \cdot 10^{-6}$	$E_c \cdot 10^{-6}$	$E_N \cdot 10^{-6}$	$E_{lim} \cdot 10^{-6}$	$E_{int} \cdot 10^{-6}$
1	4,05	4,05	4,05	4,05	4,05
2	2,64	2,64	2,64	2,49	2,32
3	0,94	1,21	1,06	0,80	0,49
4	0,19	0,24	0,21	0,16	0,10

is linear; the curve in Fig. 4b has a linear section and represents type II; the curve in Fig. 4c is of type III since it contains a linear section and the tangent at its final point is near-parallel to the deformation axis; the diagram in Fig. 4d represents type IV because it is nonlinear even at very small loads. These findings suggest that the procedure used here should be suitable for most refractories tested at any given temperature.

The elastic modulus of the materials is determined from the tangent of the angle of the tangent to the deformation curve in the coordinates $\sigma = f(\epsilon)$ at near-zero deformation. Differentiation of Eq. (4) for $\epsilon_t = 0$ gives the following equation for the extensions:

$$E_t = \frac{d\sigma_t}{d\epsilon_t} = \frac{a}{bh^2} \cdot \frac{d}{dF} \left[\left(F + \frac{1}{2} \cdot \frac{\epsilon_m}{\epsilon_t} \right) \times \left(1 + \frac{\epsilon_{cc}}{\epsilon_t} \right) \right] \frac{dF}{d\epsilon_t} = \frac{3a}{bh^2} \cdot \frac{\epsilon'_m}{(\epsilon'_t)^2} \quad (6)$$

Similarly for the compression:

$$E_c = \frac{3a}{bh^2} \cdot \frac{\epsilon'_m}{(\epsilon'_c)^2} \quad (7)$$

To evaluate this procedure and check the precision of the measurements, a comparison was made between the elastic moduli determined for given specimens by the static and dynamic methods. For steel grade St.3 the mean values are $E_{st} = 2.08 \cdot 10^6$ kg/cm² and $E_{dyn} = 2.09 \cdot 10^6$ kg/cm², and for material No. 1 $E_{st} = 4.05 \cdot 10^6$ kg/cm² and $E_{dyn} = 4.00 \cdot 10^6$ kg/cm². The elastic moduli of the materials concerned here are given in Table 2.

The equations used in earlier research for evaluating the results of bending tests can be easily derived from Eqs. (4), (6), and (7). Disregarding the difference between the tensile and compression deformation of the materials, i.e., assuming $\epsilon_t = \epsilon_c = \epsilon_m$, the following equation can be derived from Eq. (4):

$$\sigma_N = \frac{2a}{bh^2} \left(F + \frac{\epsilon_m}{2} \cdot \frac{dF}{d\epsilon_m} \right) \quad (8)$$

This equation was formulated by Nadai [6] and used by Passmore et al. [4] and Canon et al. [5]. The equation of the elastic modulus is then written as follows:

$$E_N = \frac{3a}{bh^2} \cdot \frac{dF}{d\epsilon_m} \quad (9)$$

Disregarding the nonlinearity of the deformation diagrams but assuming that the material resists extension and compression in different ways, then $\epsilon_t = \epsilon_t/F$ and $\epsilon'_c = \epsilon_c/F$, and from Eq. (4)

$$\sigma_D = \frac{3a}{bh^2} F \frac{\epsilon_m}{\epsilon_t},$$

which is the equation formulated by Duckworth [8].

Assuming the material to be linearly elastic, i.e., idealizing its deformation process as is the practice in textbooks on the strength of materials [9], equations (4) and (6) will give the equations used in engineering problems to calculate the limiting stresses:

$$\sigma_{\text{lim}} = \frac{3a}{bh^2} F \quad (10)$$

and elastic modulus:

$$E_{\text{lim}} = \frac{3a}{bh^2} \cdot \frac{F}{\varepsilon_m} \quad (11)$$

A comparison follows of the results obtained from the various approaches to the problems of determining the strength of the materials. The diagrams in Fig. 3 show that all curves of $F = F(\varepsilon_t)$ and $F = F(\varepsilon_c)$ are convex in the upward direction. It follows that

$$\frac{dF}{d\varepsilon_t} \leq \frac{F}{\varepsilon_t} \text{ and } \frac{dF}{d\varepsilon_c} \leq \frac{F}{\varepsilon_c}.$$

Using these expressions, it will be found from Eq. (8) and (10) that

$$\sigma_N = \frac{2a}{bh^2} \left(F + \frac{\varepsilon_m}{2} \cdot \frac{dF}{d\varepsilon_m} \right) \leq \frac{2a}{bh^2} \left(F + \frac{\varepsilon_m}{2} \cdot \frac{F}{\varepsilon_m} \right) = \sigma_{\text{lim}},$$

where $\sigma_N = \sigma_{\text{lim}}$ only for linearly elastic equal and dissimilar tensile and compression deformations. The diagrams in Fig. 3 show, moreover, that the $F = F(\varepsilon_t)$ curves lie to the right of those for $F = F(\varepsilon_c)$, i.e.,

$$\frac{d\varepsilon_t}{dF} \geq \frac{d\varepsilon_c}{dF}.$$

These quantities are equal only for a material with identical curves of deformation by extension and compression.

In that case, according to Eq. (4) and (8)

$$\sigma_{u,t} = \frac{a}{bh^2} \left(F + \frac{\varepsilon_m}{2} \cdot \frac{dF}{d\varepsilon_m} \right) \left(1 + \frac{\varepsilon_c}{\varepsilon_t} \right) \leq \frac{2a}{bh^2} \left(F + \frac{\varepsilon_m}{2} \cdot \frac{dF}{d\varepsilon_m} \right) = \sigma_N,$$

i.e., the quantities $\sigma_{u,t}$, σ_N , and σ_{lim} lie in the descending order as follows:

$$\sigma_{\text{lim}} \geq \sigma_N \geq \sigma_{u,t}$$

These findings were confirmed by the calculation results in Table 3 which shows the errors in the results obtained with the various equations for calculating the ultimate strength.

A comparison of Eq. (6), (7), (9), and (10) for the elastic moduli shows* that

$$E_c \geq E_N \geq E_t \geq E_{\text{int}} \text{ and } E_N \geq E_{\text{lim}} \geq E_{\text{int}},$$

These relations are illustrated by the results of calculations of the elastic modulus in Table 4.

The strength of a material can be determined not only from the force-deformation diagrams but also from the diagram of the deflection of the specimen vs the force. Since in pure bending the deflection of the beam between the outer supports is constant, according to the differential equation of the line of deflection [9, p. 124]:

$$\varepsilon_m = \frac{4h\delta}{(L-2a)^2}. \quad (12)$$

This equation does not depend on the shape of the deformation curve of the material. Using Eq. (12), Eq.

* E_{int} is the intersecting modulus, a quantity often used for practical purposes and equal to the ratio of the strength to the deformation of the material, i.e., $E_{\text{int}} = \sigma_{u,t}/\varepsilon_t$ in the present case.

(8) can be reformulated as follows:

$$\sigma_N = \frac{2a}{bh^3} \left(F + \frac{\delta}{2} \cdot \frac{dF}{d\delta} \right). \quad (13)$$

The curves $F = F(\delta)$ can be used in combination with Eqs. (12) and (13) for plotting the deformation of the material in terms of $\sigma_N = f(\varepsilon_m)$. Note that in the general case the function $F = F(\delta_1)$, where the deflection δ_1 of the specimen is measured from the level of the outer supports, cannot be used for plotting the deformation diagram $\sigma_N = f(\varepsilon_m)$ because the relation between δ_1 and ε_m depends on the shape of the deformation curve.

In the present writers' approach to the evaluation of the results of the experiment it is possible to calculate the magnitude of the measure of brittleness of the material [1] which equals the ratio of the brittle energy B of the specimen at the instant of destruction to the energy U expended on its deformation:

$$\chi = B/U.$$

This quantity can be used for assessing the behavior of the material under mechanical and thermal loads. For the present case, the brittleness values are determined from the equation

$$\chi = \frac{\sigma_{u,t}^2}{2E_t \int_0^{\varepsilon_t} \sigma_t d\varepsilon_t},$$

and are given in Table 2. The data in Tables 2 and 3 show that the discrepancy between σ_{lim} and the measured ultimate strength of the material increases as the measure of brittleness χ decreases. It follows that information relating to the strength of a material should be supplemented with the χ values which express the deformation characteristics of the material under a load.

In tests based on the principle of three-point deflection, the stress conditions of the beam depend not only on the bending moment but also on the transverse force. Moreover, as already stated, the relation between the deformation and deflection of the specimen depends on the shape of the deformation curve so that the results of three-point bending tests cannot be used for a precise determination of the strength of materials.

In spite of the relatively simple structure of Eqs. (4)-(9), the relevant calculations entail certain difficulties owing to the necessity to calculate the derivatives $d\varepsilon_t/dF$ and $d\varepsilon_c/dF$ precisely because the analytical equations for the functions $F = F(\varepsilon_t)$ and $F = F(\varepsilon_c)$ are usually unknown and the derivatives must be determined numerically. Numerical differentiation is unsuitable [10, p. 152] because a small error in the determination of the equation to be differentiated influences the value of its derivative to a significant extent. The present writers therefore used the method developed by Dolgoplova and Ivanov [11] and plotted the curve $\tilde{\varepsilon}_t(F)$ which not only approached the experimental curve $\varepsilon_t(F)$, i.e.

$$\int_0^{F_{lim}} (\varepsilon_t - \tilde{\varepsilon}_t)^2 dF \ll \eta^2,$$

but was possibly also smoother, i.e., it gave a minimized functional

$$\Phi(\tilde{\varepsilon}_t) = \int_0^{F_{lim}} (\tilde{\varepsilon}_t')^2 dF,$$

where F_{lim} is the limiting force, kg; η is the required approximation of the experimental curve.

In this case ε_t' will differ only marginally from the required derivative. The derivative $\varepsilon'(F)$ is calculated similarly. The algorithm for constructing the diagrams was programmed for a Mir-2 computer.

CONCLUSIONS

A procedure was developed and tested for evaluating the results of bending tests. In this procedure account is taken of the nonlinearity of the deformation diagrams for the material and of the difference in the resistance of brittle materials to extension and compression.

Using this procedure, it is possible to determine the true ultimate strength, the static modulus of elasticity, the limiting deformation, and the degree of brittleness of refractories from a single pure-bending test; the result being that tests can be more efficient and knowledge about the behavior of the material will be greatly increased so that it will be possible to arrive at a more accurate assessment of the service efficiency of the material when subjected to thermal effects.

The quantity σ_{lim} , which in practice is usually interpreted as the ultimate bending strength, corresponds to the true ultimate strength only for a linearly elastic material. For materials with nonlinear deformation diagrams, which include the majority of refractories, the use of σ_{lim} results in overstated strength values which is quite inadmissible for a material to be used in design analyses and estimates. The term "ultimate bending strength" as a description of the quantity σ_{lim} should obviously be replaced by, for example, the term "conditional ultimate bending strength" (by analogy with the American term "modulus of rupture").

Data about the strength of materials should be supplemented with a quantity which characterizes the deformation curve, e.g., the degree of brittleness λ .

LITERATURE CITED

1. G. A. Gogotsi, *Probl. Prochnosti*, No. 10, 26-29 (1973).
2. G. A. Gogotsi, V. V. Gotsulenko, Ya. L. Grushevskii, et al., *Zavod. Lab.*, 40, No. 11, 1407-1408 (1974).
3. V. S. Kienow and H. W. Hennieke, *Tonindustrie Zeitung*, 90, No. 12, 575-577 (1966).
4. E. Passmore, A. Moschetti, and T. Vasilos, *The Philosophical Magazine*, 13, No. 126, 1157-1162 (1966).
5. R. F. Canon, J. T. A. Roberts, and R. J. Beals, *J. Amer. Ceram. Soc.*, 54, No. 2, 105-112 (1971).
6. A. Nadai, *The Plasticity and Destruction of Solids* [Russian translation], IL, Moscow (1954).
7. G. S. Pisarenko and G. A. Gogotsi, *Ogneupory*, No. 2, 44-47 (1974).
8. W. H. Duckworth, *J. Amer. Ceram. Soc.*, 34, No. 1, 1-9 (1951).
9. S. P. Timoshenko, *Strength of Materials*, Vol. 1 [in Russian], Nauka, Moscow (1965).
10. I. S. Berezin and N. P. Shidkov, *Calculation Methods*, Vol. 1 [in Russian], Nauka, Moscow (1966).
11. T. F. Dolgopolova and V. V. Ivanov, *Zh. Vychisl. Matem. i Matem. Fiziki*, 6, No. 3, 570-576 (1964).